Applied Catalysis B: Environmental 179 (2015) 229–238

Contents lists available at ScienceDirect

Applied Catalysis B: Environmental

journal homepage: www.elsevier.com/locate/apcatb

Characterization of BiOX compounds as photocatalysts for the degradation of pharmaceuticals in water

John C. Ahern, Rebecca Fairchild, Jin Sun Thomas, Jordan Carr, Howard H. Patterson*

Chemistry Department, University of Maine, Orono, ME 04469 USA

ARTICLE INFO

Article history:
Received 4 February 2015
Received in revised form 21 March 2015
Accepted 14 April 2015
Available online 11 May 2015

Keywords:
BiOX
Photocatalysis
Pharmaceuticals
Water remediation

ABSTRACT

The surface and photophysical properties of bismuth oxyhalide catalysts were determined and correlated with photocatalytic activity. The catalysts themselves were characterized using SEM-EDS, XRD, BET and steady-state luminescence. The photocatalytic potential of these catalysts was determined for their ability to degrade 17 α-ethinyl estradiol (EE2) and estriol at the ppm level in water. The degree of photodecomposition was evaluated using luminescence spectroscopy and HPLC-MS/MS. This is the first time BiOX catalysts have been used to photodegrade synthetic estrogens. Also, this study reports that these BiOX catalysts are more effective at photocatalyzing the selected pharmaceuticals than traditional catalysts such as TiO_2. The photocatalytic mechanisms for EE2 and estriol were compared between samples treated with BiOX and TiO_2. These BiOX catalysts show great potential as solution to waste water treatment and environmental remediation.

1. Introduction

A new class of catalysts known as bismuth oxyhalides have emerged as a potentially more effective alternative to the traditional TiO_2 based catalysts [1–4]. When BiOX catalysts are exposed to UV light in water, $OH^\bullet$ and $O_2^{\bullet-}$ radicals can be formed [5]. The $OH^\bullet$ is able to oxidize organic compounds to form products that in some cases will degrade more easily under UV light [5]. One advantage of BiOX catalysts over TiO_2 is their smaller band gap. BiOI and BiOCl have band gaps of 1.76 eV and 3.19 eV, respectively [6]; whereas, TiO_2 has a band gap of 3.20 eV [3]. This allows the BiOX catalysts to function under near UV and even visible light sources unlike TiO_2 which requires UV light to function [7]. Bismuth oxyhalides including BiOCl and BiOI were tested as photocatalysts for the degradation of two different pharmaceuticals in deionized water. These catalysts were compared to more conventional catalysts including TiO_2. The synthetic estrogens: 17α-ethinyl estradiol and estriol were selected as model compounds for study because they are of concern to federal and state environmental protection agencies and EPA [8–14]. The degradation rates and mechanisms were compared based on catalyst type. This is the first time BiOX catalysts have been used to photodegrade synthetic estrogens.

Endocrine disrupting chemicals like EE2 and estriol have an adverse effect on organisms at even low concentrations [13,15]. These compounds can be transported through surface and ground water hundreds and thousands of kilometers away causing harm to the environment [16–19]. EE2 and estriol mimic natural estradiol and they can bind to estrogen receptors. EE2 is used by over 104 million women as a contraceptive [13]. Fish are among the most critically exposed group and also present the most sensitive group for adverse effects of endocrine disruption [15,20,21]. Long-term exposure to doses as low as 5 ng EE2 can lead to infertility in male zebrafish [13]. These compounds have been detected at sewage treatment plants as well as in drinking water. There is a need to effectively degrade them. TiO_2 has been studied as a means of degrading EE2 but a prolonged exposure (over 1 h) and/or use of a high energy (254 nm) UV source were required [4,22–24]. The kinetic mechanisms for the photocatalysis of the estrogens will provide essential knowledge on how BiOX catalysts interact with estrogens and related compounds.

The synthesis method for the BiOX catalysts was chosen because it is fast, simple and affordable. A \$20 bottle of 10 g of $NaBiO_3$ can be used to successfully make about 4 g of BiOCl or 6 g of BiOI which is enough for over 200 experiments of the type used in this paper. The catalysts can be prepared in just a few steps, and they are ready for use within 7 h, 6 of which are for drying in an oven. The purity

* Corresponding author. Tel.: +1 207 581 1178; fax: +1 207 581 1191.
E-mail address: howardp@maine.edu (H.H. Patterson).

http://dx.doi.org/10.1016/j.apcatb.2015.04.025
0926-3373/

of the BiOCl and the BiOI catalysts compare well to BiOX catalysts prepared by others [2].

The BiOX catalysts themselves were characterized using a variety of methods. First, the BiOX catalysts were analyzed using scanning electron microscopy electron dispersive X-ray spectroscopy (SEM-EDS) to better understand their surface properties and determine their elemental composition. Then, the catalysts were analyzed using Brunauer–Emmett–Teller (BET) analysis and X-ray diffraction (XRD) to determine surface area and phase identity, respectively. The catalysts were also analyzed using steady-state luminescence spectroscopy to help define their photophysical properties. The results of all of these physical and photophysical methods were then correlated with the results of the photocatalysis experiments, principally liquid-phase luminescence spectroscopy.

Liquid-phase luminescence spectroscopy, specifically Excitation Emission Matrix (EEM) spectroscopy as the principle method used in this study for evaluating pharmaceutical concentration. EEM scans are 3-dimensional luminescence scans with excitation on the *x* axis, emission on the *y* axis and intensity of the emission on the *z* axis. EEMs allow for a series of emission scans to be taken of a sample at different excitation energies. This allows for a complete image of the luminescence properties of the compound of interest. The Patterson research group and others have successfully used luminescence spectroscopy including EEMs to track water pollutant concentration including phenol and indole [25–35]. EEM spectroscopy was chosen in this study to determine pharmaceutical concentration because it has proven as a rapid and accurate means of detecting organic pollutants in water [27,30,32–34].

High-performance liquid chromatography tandem mass spectrometry (HPLC-MS/MS) was used to develop mechanisms for the degradation of the two pharmaceuticals in water. The peaks in the spectra were used to identify major ionized fragments that correspond to individual degradation products. These identified products were then used to assist in constructing a logical mechanism for the degradation of the starting pharmaceutical compound. This process was done for each pharmaceutical with each catalyst at various UV exposure time intervals between 0 and 30 min. HPLC-MS/MS is a favored choice for mechanism development because there is no need for solvent extraction that remove or complex with degradation products. The particular HPLC-MS/MS method has been successfully used by the Patterson group and others for pharmaceuticals and other organics in water [4,8,36–40]. The mechanisms for the degradation of each pharmaceutical were compared based on catalyst type and duration of UV exposure. The degree of photodecomposition exhibited in the mechanisms for each catalyst type and UV exposure time were used in conjunction with the liquid-phase luminescence results to evaluate catalyst performance.

2. Experimental

2.1. Catalyst synthesis

2.1.1. BiOX (where X = Cl or I)

Composites of BiOCl were formed. This catalyst was made by dissolving $NaBiO_3$ in a 21 ml 2:1 mixture of ethanol:DI water followed by adding 6 ml of 15% weight by volume HCl and stirring. The solid was then allowed to settle out of solution and the liquor was decanted off. The white paste like solid was then vacuum filtered and washed with ethanol. Finally, the solid was baked at 80 °C in an oven for 6 h. The final result was a flaky, white compound. The sample should be over 99% pure given the amount of HCl used in similar studies [5]. The same procedure was conducted to create BiOI except 6 ml of 7.5% weight by volume, HI was used instead of HCl. The resulting solid was dark orange.

2.1.2. TiO_2

Titanium dioxide TiO_2 (P25) was purchased from Degussa Corporation, Germany and used as acquired.

2.2. Surface characterization methods

2.2.1. SEM-EDS analysis

Scanning electron microscopy electron dispersive X-ray spectroscopy (SEM-EDS) was used to characterize the morphology and elemental composition of the catalysts. SEM-EDS scans were conducted using a Zeiss SII Nvision 40 SEM with Ametek EDAX Genesis EDS mounted on it. The SEM image was done at a working distance of 4.4 mm and an EHT value of 6.31 kV. The EDS was run at 7.0 kV. The EDS results were used to evaluate elemental composition of crystals of the catalysts.

2.2.2. BET analysis

Brunauer–Emmett–Teller (BET) analysis was used to determine the specific surface area of the catalysts. The isotherms were measured on a micromeritics ASAP 2020 BET system at 77 K.

2.2.3. XRD analysis

X-ray Diffraction (XRD) scans were done on the BiOX catalysts to verify the composition purity and crystallinity of the compounds. The prepared samples were characterized by a X-ray diffractometer (X'pert Pro PANalytical & Gonio pixcel) operated with a CuKα line at 45 kV of an acceleration voltage and 40 mA of a current.

2.2.4. DLS analysis

Dynamic light scattering (DLS) scans were recorded to measure any changes in morphology of the catalysts pre and post exposure to UV radiation. The scans were done using a Malvern Nano Range Zetasizer over a range of 0.4 nm–10 μm.

2.3. Steady-state luminescence and luminescence lifetimes

Steady-state luminescence scans were run on the BiOI and BiOCl at 78 K. Spectra were collected with a Model Quantamaster-1046 photoluminescence spectrometer from Photon Technology International. This device utilizes a 75 W xenon arc lamp coupled with two excitation monochromators and one emission monochromator to adjust the bandwidth of light hitting the sample and detector, respectively. Light intensity was measured using a photomultiplier tube. The samples were mounted on a copper plate using a non-emitting copper-dust-high vacuum grease. The spectra were run sequentially with an excitation of 500 nm down to 200 nm as a batch scan. Emission was monitored over a wide band from 230 nm to 530 nm. The resulting scans form a 3-d matrix with excitation as the *x* axis, emission on the *y* axis, and intensity on the *z* axis. The wavelength of the exciting light was run from low to high wavelength to avoid photobleaching, oxidation or other forms of degradation. Low-temperature scans were run on the same system coupled to a Janis ST-100 optical cryostat. Liquid nitrogen and liquid helium were used as coolants.

Luminescence lifetime measurements were collected by exciting the BiOX samples using an Opotek 355 II Tunable laser operating at 300 nm. The emissions were collected using a Jobin Yvon Ramanor system, and the lifetime was read with a LeCroy oscilloscope, collecting data every 10 ns for 50 μs per sweep, averaging 1000 sweeps per sample. Emission was monitored at 419 nm for the BiOI sample and 422 nm and 456 nm for the BiOCl which correspond with their emission maxima from the steady-state luminescence study. The excitation energy of 300 nm was chosen

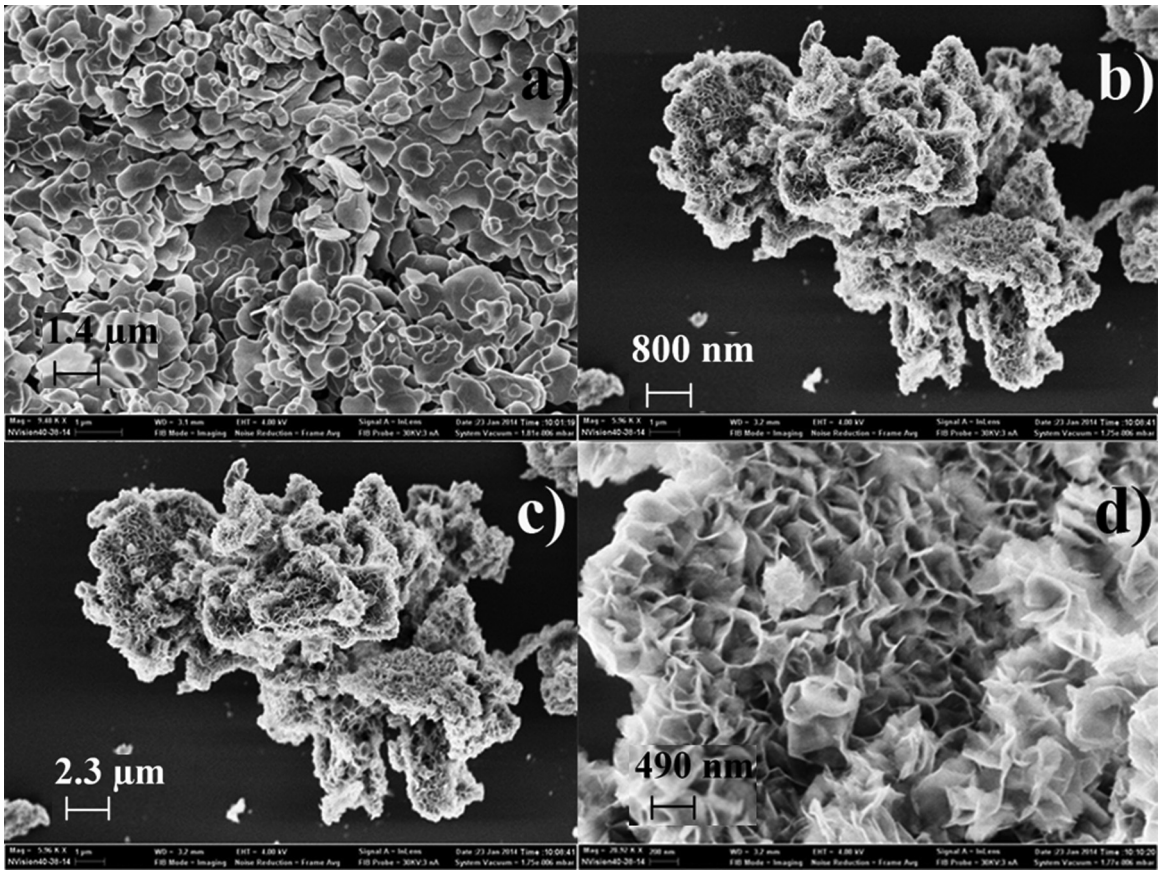

Fig. 1. SEM images of (a) BiOCl clusters at 9.48 e^3 magnification. View window is 12.5 µm × 8.75 µm. (b) Single BiOCl cluster at 16.6 e^3 magnification. View window is 7 µm × 4.8 µm. (c) BiOI clusters at 5.96 e^3 magnification. View window is 20.3 µm × 14.3 µm. (d) Single BiOI cluster at 28.9 e^3 magnification. View window is 4.3 µm × 3 µm.

because the laser emits effectively at this wavelength and both of the samples can be effectively excited at that wavelength. All luminescence lifetime scans were run at 77 K using liquid nitrogen as a coolant.

2.4. Photocatalysis and liquid-state luminescence experiments

Photodegradation experiments using 17α-ethinyl estradiol (EE2) and estriol as model compounds were conducted by creating 0.0500 l 10.000 mg/l solutions of each in DI water and pouring them into quartz flasks. Catalysts (either BiOX or TiO_2) were added to the mixture at a concentration of 0.5 g/l and stirred for 3 h in darkness. The slurry was then transferred to a quartz round bottom flask and irradiated using either sixteen 68 W/m^2 350 nm bulbs or four 128 W/m^2 254 nm bulbs arranged in a circle. Aliquots were taken at given time intervals between 0 min and 30 min and put in separate vials. The quartz flasks were continuously stirred while being irradiated. The contents of the vials were filtered using a 0.20 µm syringe filter prior to concentration determination. The scans were done on a Jobin Yvon Horiba Fluorolog 3 with cuvettes from Starna Cell made from far UV quartz. The excitation window was 250–300 nm with an offset of 3 nm between each scan and the emission window was 285–350 nm with an offset of 3 nm. The slit widths were kept constant at 5 nm on the excitation side and 5 nm on the emission side. The sample scans were normalized to a water Raman scan to account for variances in lamp intensity from day to day. Signal contribution from water and the catalysts was blank subtracted from the sample scans. The pH of the solution was determined for each UV exposure time interval for each catalyst using a Hach pH probe.

2.5. HPLC-MS/MS experiments

Samples of EE2 and estriol in water post catalyst and UV treatment were scanned using high performance liquid chromatography tandem mass spectrometry (HPLC-MS/MS). This was done to identify the degradation products and construct mechanisms for EE2 and estriol photocatalysis. The samples were analyzed using a 6530 high performance liquid chromatographic-chip quadrupole time-of-flight mass spectrometer (HPLC-Chip/Q- TOFMS; Agilent Technologies, Santa Clara, CA).

3. Results and discussion

3.1. Surface characterization

3.1.1. Scanning electron microscopy

Scanning electron microscope (SEM) images were collected for the BiOI and BiOCl catalysts. The images provide insight on the morphology and composition of the surface of the BiOX catalysts. Fig. 1a shows an aggregation of BiOCl platelet clusters. Fig. 1b is a view of a single cluster of BiOCl at high magnification. Fig1c shows an aggregation of BiOI clusters, and Fig. 1d is a single cluster of BiOI at high magnification. The size of the platelets is highly variable, ranging from 200 nm to 1 µm in diameter and 10 nm to 100 nm in thickness.

Electron dispersive X-ray spectroscopy (EDS) was used in conjunction with the SEM to determine elemental composition of the BiOX catalysts. The sample of both the BiOI and BiOCl was found to be pure, and the ratio of detected elements were in agreement with the BiOX formula. The results of the EDS study can be seen in the supporting information in Figs. S1 and S2 and Tables S1 and S2. Each of the major peaks in the graph is identified with labels and

Table 1
Properties of various catalysts.

Catalyst type	Surface area (m^2)
BiOCl	2.677
BiOI	11.07
TiO_2	50.0

the peak areas were used to determine percent composition which is presented in the tables.

3.1.2. BET analysis results

Table 1 gives a comparison of the specific surface area for the various catalysts. Figs. S3 and S4 depict the isotherms for BiOCl and BiOI, respectively. The higher surface area of the TiO_2 may make it more effective for pharmaceutical removal pre-UV exposure. However, this advantage is quickly lost after just a couple minutes of UV exposure. Also, the pharmaceuticals that were adsorbed onto the TiO_2 surface were not necessarily decomposed. The BiOX catalysts are more effective catalysts than TiO_2 despite having lower surface area than TiO_2 because they have more active surface sites. This is due is part because of their lower band gap which allows their surface sites to be activated given lower energy irradiation. Also, their active sites may be re-usable more times than those of TiO_2.

3.1.3. XRD analysis results

Fig. 2 shows the XRD patterns for the BiOX catalysts. The spectra for both the BiOI and BiOCl indicate single platelet phase for each catalyst type. The position and the narrowness of the peaks indicate uniformly tetragonal crystalline structure and compare well with previously published works on pure crystals of BiOX compounds [3,41]. This is further evidence of the uniformity and purity of the catalysts studied.

3.1.4. DLS analysis results

Dynamic light scattering (DLS) results for both BiOCl and BiOI pre and post exposure to UV radiation showed no significant change in particle size distribution. Figs. S5 and S6 show the DLS spectra.

3.2. Steady-state luminescence results

Both the BiOCl and BiOI were characterized using steady state luminescence at 77 K. The BiOX catalysts do not emit at temperatures above 90 K. Figs. 3 and 4 show the steady state luminescence spectra for BiOI and BiOCl, respectively. The annotations with arrows above the peaks indicate the excitation/emission energy that corresponds with the emission/excitation peaks, respectively. The BiOI exhibited a single broad emission band centered at 419 nm given a relatively low energy excitation of 381 nm with a Stokes Shift of 2380 cm^{-1}. The luminescence lifetime of this emission was 21.8 μs. The BiOCl had two emission bands, one high energy at 422 nm and one low energy at 456 nm and with excitations

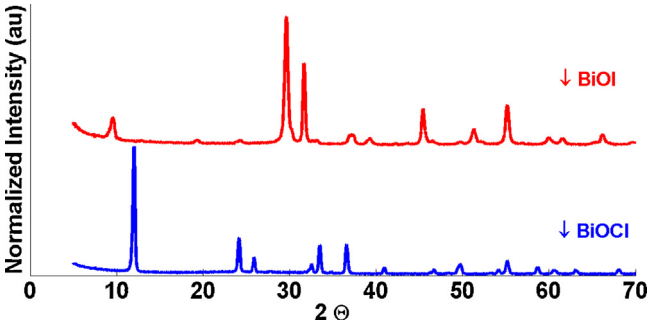

Fig. 2. XRD patterns for BiOI and BiOCl.

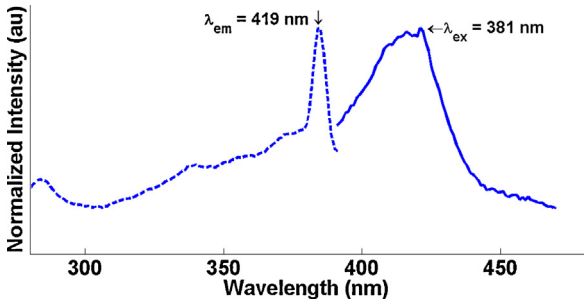

Fig. 3. Steady state luminescence spectra for BiOI at 77 K. The annotations with arrows indicate the excitation/emission energy that corresponds with the selected emission/excitation peaks, respectively.

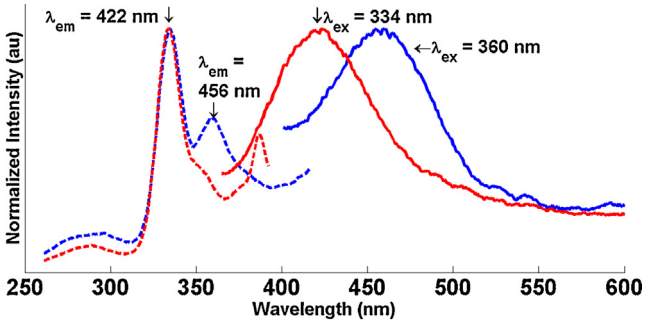

Fig. 4. Steady state luminescence spectra for BiOCl at 77 K. The annotations with arrows indicate the excitation/emission energy that corresponds with the selected emission/excitation peaks, respectively.

of 334 nm and 360 nm, respectively. Table 2 shows the assignments for the peaks from BiOCl. For both the BiOCl and BiOI, the emissions were likely caused by relaxation of the excited lattice via phonon–phonon interactions [42,43]. The luminescence lifetimes (3.82–23.2 μs) indicate a phosphorescent reaction. This is in agreement with similar studies [42]. The BiOCl has two possible emissions because it has a high-energy excited state and a low-energy excited state corresponding with the high and low energy emission, respectively. In each case, the photo-excited Bi induces a photo-generated hole which can directly degrade the organic or react with OH^- or O_2 to form the respective radicals $OH^\bullet$ or $O_2^{\bullet-}$ which can bind to the organic and allow it to cleave more easily [6].

3.3. Photocatalysis and liquid-phase luminescence experiments

Fig. 5 and Table 3 show enhanced degradation of EE2 under 350 nm UV light for BiOX treated samples versus TiO_2 treated ones. Both of the BiOX catalysts performed better than TiO_2. The BiOI catalyst proved to be the most effective given 30 min of 350 nm UV exposure. Most of the catalysts adsorbed a portion of the pharmaceuticals onto their surface. This accounts for the sub-100% EE2 level pictured in Tables 4 and 5 even at 0 min of UV exposure. The pH did not vary much for most of the different catalyst treated samples of EE2 under 350 nm UV exposure. The TiO_2 treated samples were the exception. The pH of TiO_2 treated samples decreased from around 6.5 at 0 min of UV exposure to about 2.9 after 30 min of UV exposure. This is because TiO_2 is effective at producing hydroxyl radicals, which induces the propagation of H^+ ions, which in turn,

Table 2
Observed emission maxima for BiOCl at 77 K.

λ_{em} (nm), [λ_{ex} (nm)]	Stokes shifts (cm^{-1})	Lifetime (μs)
422, [334]	6240	23.2
456, [360]	5850	3.82

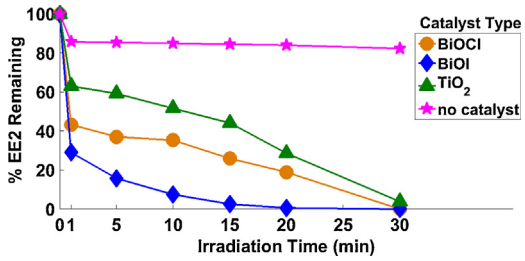

Fig. 5. Percent of EE2 remaining in solution in the presence of various catalysts under 350 nm UV light. The points at time zero are pictured exclusively for pre-adsorption for clarity. The post adsorption data is pictured in Table 3.

Table 3
Percent of EE2 remaining after treatment with different catalysts and 350 nm UV as determined via EEM spectroscopy. Initial concentration of EE2 was 10.000 mg/l. Experiments were conducted three times and the results were averaged to generate this table.

Catalyst	0 min UV (pre Ads.)	0 min UV (post Ads.)	20 min UV	30 min UV
BiOCl	100	46.0	18.9	0[a]
BiOI	100	38.1	0.607	0[a]
TiO_2	100	68.1	28.7	3.85
No catalyst	100	100	84.1	82.4

[a] Signal intensity was 0 but concentrations cannot be discerned from one another below 7.00 μg/l.

decrease pH [4]. A table of pH change as a function of UV exposure time for solutions of EE2 can be seen in Supplementary information in Table S3.

Fig. S7 is a plot of ln(% EE2 Remaining) versus 350 nm light exposure time. The plot for the first 20 min of exposure time is linear indicating 1st order degradation kinetics. However, after 20 min the reaction rate for BiOCl and BiOI treated samples becomes non-linear with a second, faster reaction occurring. At 20 min of UV exposure the percent EE2 remaining is 18.9% for BiOCl-treated samples and 0.607% for BiOI-treated samples.

High energy UV light (254 nm) was also tested as an energy source for photocatalysis. Fig. 6 and Table 4 show enhanced degradation of EE2 under 254 nm UV light for BiOX treated samples versus TiO_2 treated ones. Once again, the BIOX catalysts were more effective at reducing the concentration of EE2. The BiOCl catalyst proved to be the most effective given 30 min of 254 nm UV exposure. The photodegradation of EE2 increases with an increase in energy as can be seen when comparing the results for 350 nm and 254 nm exposure. The performance of TiO_2 increases a great deal between 350 nm and 254 nm because the higher energy is able to bridge the band gap to allow the catalysts to function. The BiOX catalysts are more effective than TiO_2 at both irradiation energies; however, because of the smaller band gaps for BiOX, the additional UV energy does not make as large of a difference in performance. Also, the higher energy UV light allows for more direct photolysis.

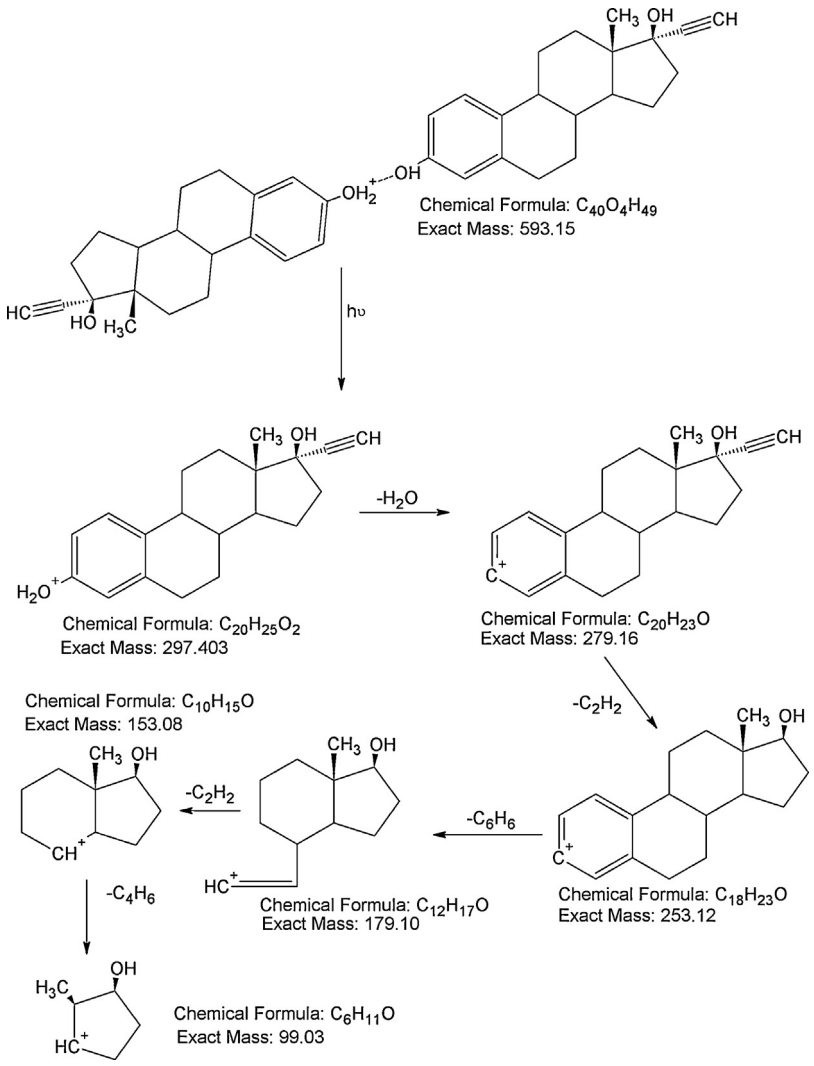

Scheme 1. Mechanism for direct photolysis of EE2 using BiOI and 350 nm UV.

Table 4
Percent of EE2 remaining after treatment with different catalysts and 254 nm UV as determined via EEM spectroscopy. Initial concentration of EE2 was 10.000 mg/l. Experiments were conducted three times and the results were averaged to generate this table.

Catalyst	0 min UV (pre Ads.)	0 min UV (post Ads.)	20 min UV	30 min UV
BiOCl	100	38.2	2.62	0[a]
BiOI	100	66.3	2.23	0.404
TiO_2	100	40.3	10.5	1.55
No catalyst	100	100	33.9	27.4

[a] Signal intensity was 0 but concentrations cannot be discerned from one another below 7.00 μg/l.

Table 5
Percent of estriol remaining after treatment with different catalysts and 350 nm UV as determined via EEM spectroscopy. Initial concentration of estriol was 10.000 mg/l. Experiments were conducted three times and the results were averaged to generate this table.

Catalyst	0 min UV (pre Ads.)	0 min UV (post Ads.)	20 min UV	30 min UV
BiOCl	100	66.0	22.3	8.50
BiOI	100	74.9	18.5	0[a]
TiO_2	100	73.4	53.2	40.0
No catalyst	100	100	68.0	67.5

[a] Signal intensity was 0 but concentrations cannot be discerned from one another below 7.00 μg/l.

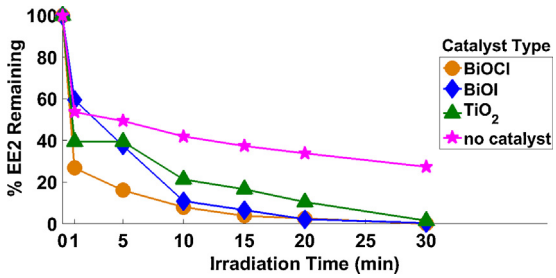

Fig. 6. Percent EE2 remaining in solution in the presence of various catalysts under 254 nm UV light. The points at time zero are pictured exclusively for pre-adsorption for clarity. The post adsorption data is pictured in Table 4.

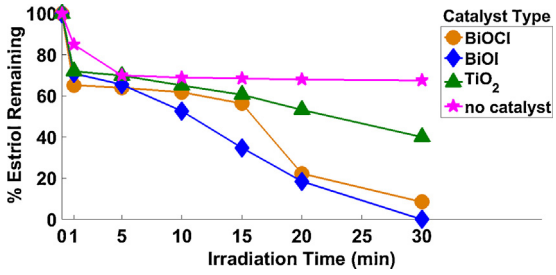

Fig. 7. Percent estriol remaining versus time plot for estriol in the presence of various catalysts under 350 nm UV light. The points at time zero are pictured exclusively for pre-adsorption for clarity. The post adsorption data is pictured in Table 5.

Fig. S8 shows a plot of ln(% EE2 remaining in solution) versus 254 nm light exposure time. The plots for all catalysts except BiOCl follows a straight line indicating 1st order degradation kinetics. After 20 min the BiOCl linear plot with only 2.63% sample remaining, becomes non-linear indicating a second reaction is also present.

The trends in catalyst performance for the photodecomposition of estriol were similar to those of EE2. Fig. 7 and Table 5 show enhanced degradation of estriol under 350 nm UV light for BiOX treated samples versus TiO_2 treated ones. The BiOI catalyst proved to be the most effective given 30 min of 350 nm UV exposure. This

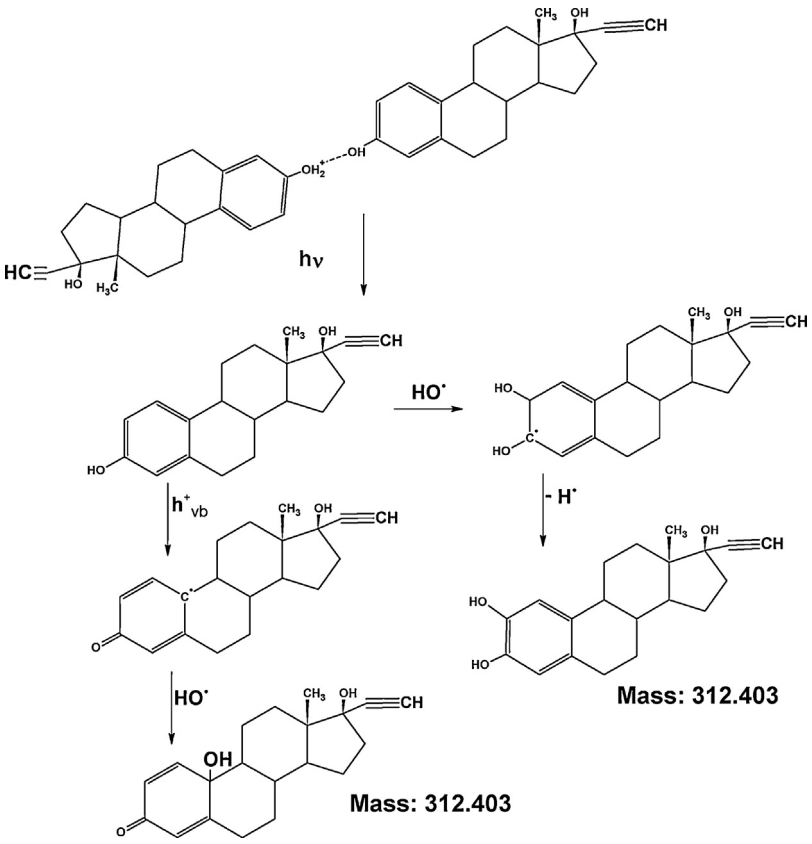

Scheme 2. Mechanism for photocatalysis of EE2 (reaction with holes as well as radicals) using BiOI and 350 nm UV.

Table 6
Percent of estriol remaining after treatment with different catalysts and 254 nm UV as determined via EEM spectroscopy. Initial concentration of estriol was 10.000 mg/l. Experiments were conducted three times and the results were averaged to generate this table.

Catalyst	0 min UV (pre Ads.)	0 min UV (post Ads.)	20 min UV	30 min UV
BiOCl	100	78.1	26.7	0[a]
BiOI	100	66.5	12.6	0.838
TiO_2	100	68.3	40.5	0[a]
No catalyst	100	100	46.7	38.1

[a] Signal intensity was 0 but concentrations cannot be discerned from one another below 7.00 μg/l.

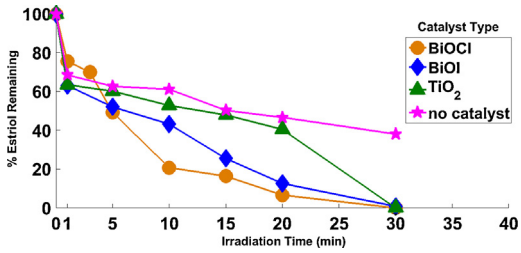

Fig. 8. Percent estriol remaining versus time plot for estriol in the presence of various catalysts under 254 nm UV light. The points at time zero are pictured exclusively for pre-adsorption for clarity. The post adsorption data is pictured in Table 6.

is likely because of the smaller band gap for BiOI. Both of the BiOX catalysts performed the best after 5 min of irradiation time. Most of the catalysts adsorbed a portion of the pharmaceuticals onto their surface. This accounts for the sub-100% estriol readings in Table 6 even at 0 min of UV exposure. The pH did not vary much for most of the different catalyst treated samples of estriol under 350 nm UV exposure. The TiO_2 treated samples were once again, the exception. The pH of TiO_2 treated samples decreased from around 6.4 at 0 min of UV exposure to about 2.9 after 30 min of UV exposure. Again, this is because TiO_2 promotes the production of hydroxyl radicals that generate H^+ ions, which decrease pH [4]. A table of pH as a function of UV exposure for solutions of estriol can be seen in the supplementary information in Table S4.

The reduction in ln(% estriol remaining) over time for most of the catalysts follows a straight line indicating 1st order degradation kinetics. Similar to EE2, Fig. S9 is a plot of ln(% estriol remaining) versus 350 nm light exposure time. The percent of estriol remaining after 20 min of UV exposure is 18.5% for BiOI-treated samples. Similar to EE2, the linear plot for BiOI treated-samples becomes non-linear after 20 min of UV exposure indicating a faster, second reaction.

The most effective catalyst for degradation of estriol at 254 nm was BiOCl, unlike when using a 350 nm light source. Fig. 8 and Table 6 show enhanced degradation of estriol under 254 nm UV light for BiOX treated samples versus TiO_2 treated ones. The BiOCl catalyst proved to be the most effective given 30 min of 254 nm UV exposure. Both BiOCl and BiOI performed especially well compared to TiO_2 for the first 20 min. Much like with EE2, the photodegradation of estriol increases with an increase in energy due in part because of an increase in direct photolysis. Also, once again the photocatalytic performance of TiO_2 increased more than BiOX going

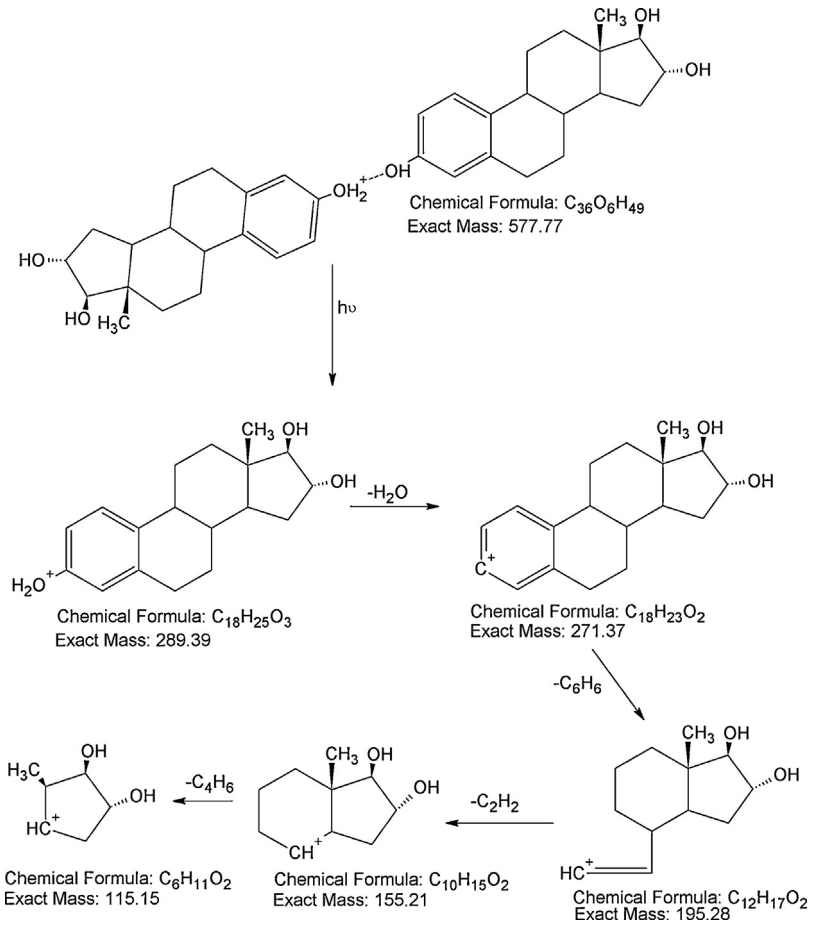

Scheme 3. Mechanism for direct photolysis of estriol using BiOI and 350 nm UV.

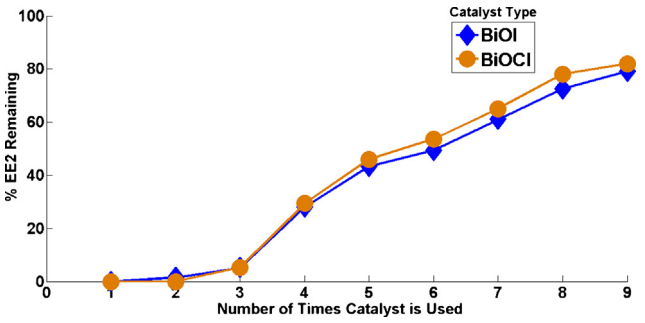

Fig. 9. Determination of number of times catalyst can be used by measuring EE2 concentration after multiple uses. Starting EE2 concentration was 10 mg/l.

from 350 nm to 254 nm exposure because of the larger band gap of TiO_2.

The reduction in ln(% estriol remaining in solution) over time for most of the catalysts indicated 1st order degradation kinetics. Fig. S10 is a plot of ln(% estriol remaining) versus 254 nm light exposure time.

Catalyst recycling: The number of times a catalyst can be used was determined to be 8 for both BiOX catalysts. This study used a fresh batch of 10 mg/l EE2 for each use of the catalyst. The catalyst concentration was 0.5 g/l. Each round of UV exposure was conducted using sixteen 68 W^2 lamps operating at 350 nm for 30 min. The samples were continuously stirred while under UV irradiation. The catalysts were filtered out of solution after each exposure and dried in an oven at 80 °C for 5 h before being used again. Fig. 9 shows how concentration increases with each re-use of the BiOX catalysts. The number of times each BiOX catalyst can be used is 8 because after being used 9 times, each catalyst performs no better than UV alone (30 min of UV treatment without any catalyst reduced the UV concentration by only 17.6%). The BiOI performed marginally better than the BiOCl after being used multiple times. The decrease in performance over time is likely because of adsorption of pharmaceuticals and their degradation products onto the surface of the catalysts thereby, reducing the effective surface area for catalysis. The number of times the BiOX catalysts can be used surpasses those of more traditional catalysts such as the previously published work using TiO_2 doped LSX zeolite which can only be used 2 times [4].

3.4. HPLC-MS/MS experiments

Results from HPLC-MS/MS experiments support the luminescence results. Ionized fragments were identified in the MS spectra as corresponding with photodegradation products that were used to construct the degradation mechanisms for each of the pharmaceuticals examined. The signals for the protonated EE2 and estriol fragments decrease in intensity with addition of BiOX catalysts and additional UV time. Also, degradation products for the EE2 and estriol were identified. Scheme 1 shows the proposed mechanism for the degradation of EE2 via direct photolysis. Scheme 2 shows a proposed mechanism for the BiOI-assisted photocatalysis of EE2 via a combination of direct reaction with the photo-induced electron–holes and OH• radical attack. Schemes 3 and 4 show the same types of mechanisms for estriol. The direct reaction with holes and radical-induced attack mechanisms pictured in Schemes 2 and 4 could be extended to include further degradation to yield small fragments similar to those pictured in Schemes 1 and 2. These mechanisms are presented in truncated form to show the differences between photocatalysis and direct photolysis. There were notably fewer pathways and degradation products for the degradation of EE2 using BiOX catalysts than

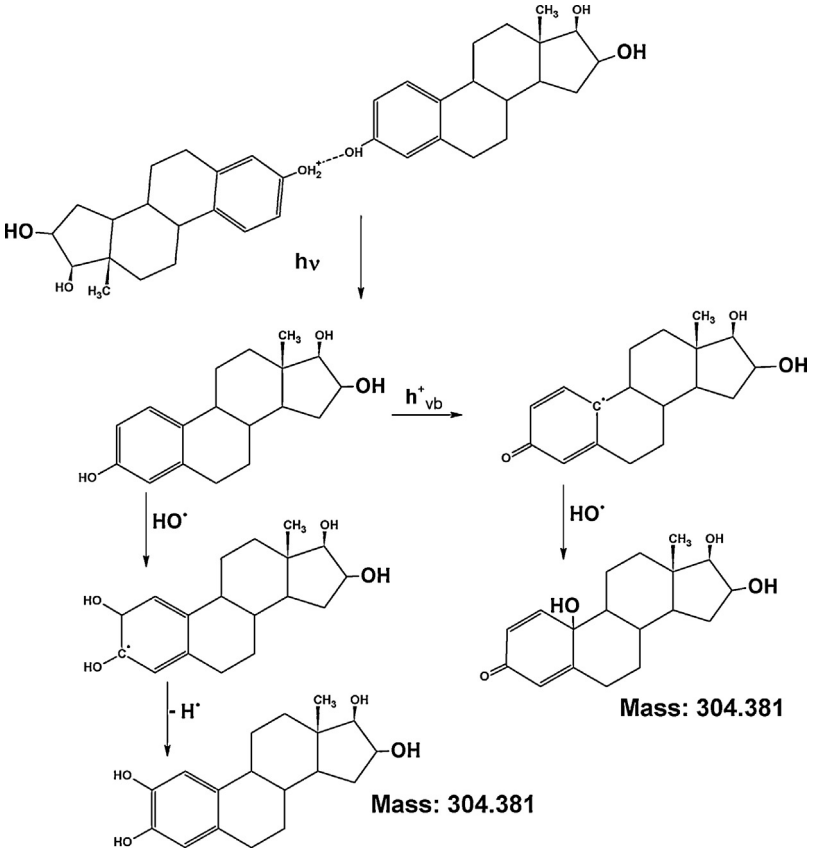

Scheme 4. Mechanism for of estriol (reaction with holes as well as radicals) using BiOI and 350 nm UV.

in the previously published work on TiO_2-doped zeolite [4]. The simpler mechanism for BiOX catalysts can allow for faster and more complete degradation of the pharmaceutical contaminant. Also, for BiOX-treated samples of both EE2 and Estriol, the ratio between small and large degradation products increases with UV exposure time. These smaller degradation products may be easier to break down, or react with the starting compound, to accelerate photocatalysis. This is in agreement with the luminescence results that show an increase in degradation rate after 20 min. The LC–MS results are complimentary to the luminescence spectra and support the claim that BiOX catalysts are the preferred choice for degradation of EE2, estriol and related pharmaceuticals. Part of the reason the degradation rate was faster for BiOX-treated samples versus the previously published doped-zeolite-treated samples is because the surface of the BiOX catalysts is entirely active. Whereas, the surface of the zeolites is merely doped with the active catalysts, and the cage structure of the zeolites can actually inhibit complete degradation [4]. Fig. S11 shows an HPLC-MS/MS spectra utilized to derive the mechanism. Fig. S12 shows an HPLC-MS/MS spectra used to determine the estriol mechanism. Figs. S13 and S14 show HPLC-MS/MS spectra for BiOI treated EE2 and estriol given longer UV exposure times. There was no significant difference in HPLC-MS/MS results/mechanisms between BiOI and BiOCl for EE2 or estriol except for the fact that BiOI tended to induce faster reduction in concentration of the starting compound and its degradation products. The HPLC-MS/MS spectra for samples with higher UV exposure times had a higher portion of small degradation products indicating more complete photodecomposition. The energy of UV irradiation (254 nm or 350 nm) did not change the possible mechanisms; however, the higher energy source likely increased the ratio between direct photolysis pathways and photocatalysis pathways. The relatively simple mechanisms coupled with the increased degradation rates for samples treated with BiOX indicate that BiOX was more effective at degrading EE2 and estriol in water than other catalysts such as TiO_2.

4. Conclusions

Bismuth oxyhalide catalysts were found to be more effective at photocatalyzing EE2 and estriol than TiO_2. BiOI was the best catalyst tested using the 350 nm light source, and BiOCl was the best catalyst using the 254 nm light source. The BiOX catalysts performed especially well compared to TiO_2 at the relatively lower UV energy (350 nm). HPLC-MS/MS was used to confirm the luminescence results and to derive mechanisms for degradation of both EE2 and estriol. This is the first time BiOX catalysts have been studied as photocatalysts for estrogens in water. The mechanisms derived in this study for EE2 and estriol are important for understanding how these new BiOX catalysts interact with related pharmaceuticals. The physical and photophysical analyses of the BiOX catalysts including SEM-EDS, XRD and BET indicate pure, uniphase photoactive catalysts with enough surface area to interact with organics. The steady-state luminescence results also confirm the catalyst identity and indicate how they can be photo-activated. The catalyst recycling experiments show that these catalysts can be effectively re-used many more times than conventional catalysts such as zeolites. These measurements along with the positive photocatalysis results support the claim that BiOX compounds are the superior catalyst for degradation of pharmaceuticals and related organics in water. The synthetic estrogens 17α-ethinyl estradiol (EE2) and estriol pose a serious risk to the biota of natural waters. The findings of this study are important because having a catalyst capable of working under low energy or even ambient light conditions reduces the cost for their use in wastewater treatment facilities.

Acknowledgments

This work was supported by the Maine Economic Improvement Fund and the National Science Foundation (Award ID: MRI 1126657) and the United States Geological Society/Water Resources Research Institute (Project #2013ME293B). JCA and HHP would like to thank Elizabeth Stemmler of Bowdoin College for running the HPLC-MS/MS. JCA and HHP would like to thank Aileen Co. for running the DLS analysis. JCA and HHP would also like to thank Aria Amirbahman of the University of Maine for allowing the use of his photochamber.

Appendix A. Supplementary data

Supplementary data associated with this article can be found, in the online version, at http://dx.doi.org/10.1016/j.apcatb.2015.04.025

References

[1] H. Park, A. Bakh, Y.Y. Ahn, J. Choi, M.R. Hoffmann, J. Hazard. Mater. 47 (2012) 211–212.
[2] X. Zhang, Z. Ai, F. Jia, L. Zhang, J. Phys. Chem. C (2008) 747.
[3] X. Chang, J. Huang, C. Cheng, Q. Sui, W. Sha, G. Ji, S. Deng, G. Yu, Catal. Commun. 11 (2010) 460.
[4] Z. Pan, E. a. Stemmler, H.J. Cho, W. Fan, L. a. LeBlanc, H.H. Patterson, A. Amirbahman, J. Hazard. Mater. 279 (2014) 17.
[5] X. Chang, G. Yu, J. Huang, Z. Li, S. Zhu, P. Yu, C. Cheng, S. Deng, G. Ji, Catal. Today 153 (2010) 193.
[6] X. Chang, J. Huang, Q. Tan, M. Wang, G. Ji, S. Deng, G. Yu, Catal. Commun. 10 (2009) 1957.
[7] X. Chang, J. Huang, C. Cheng, W. Sha, X. Li, G. Ji, S. Deng, G. Yu, J. Hazard. Mater. 173 (2010) 765.
[8] R. Hannah, V. D'Aco, P. Anderson, M. Buzby, D. Caldwell, V. Cunningham, J. Ericson, A. Johnson, N. Parke, J. Samuelian, J. Sumpter, Environ. Toxicol. Chem. 28 (2009) 2725.
[9] A.L. Filby, K.L. Thorpe, C.R. Tyler, J. Mol. Endocrinol. 37 (2006) 121.
[10] A. Kumar, I. Xagoraraki, Sci. Total Environ. 408 (2010) 5972.
[11] G.-G. Yin, R.S. Kookana, Y.-J. Ru, Environ. Int. 28 (2002) 545.
[12] P. Hallgren, A. Nicolle, L.-A. Hansson, C. Brönmark, L. Nikoleris, M. Hyder, A. Persson, Environ. Toxicol. Chem. 33 (2014) 930.
[13] P. Burkhardt-holm, Linking Water Quality to Human Health and Environment : the Fate of Micropollutants, Inst. Water Policy Natl. Univ. Singapore (2011) 1–62, August.
[14] E.M. Ferguson, M. Allinson, G. Allinson, S.E. Swearer, K.L. Hassell, P.P. Bay, Water Res. 47 (2012) 1604.
[15] K.L. Thorpe, R.O.B.I. Cummings, T.H. Hutchinson, M. Scholze, G. Brighty, J.P. Sumpter, C.R. Tyler, Environ. Sci. Technol. 37 (2003) 1142.
[16] Q. Chen, J. Shi, X. Liu, W. Wu, B. Liu, H. Zhang, J. Contam. Hydrol. 146 (2013) 51.
[17] W.J.P. Langston, G.R. Burt, B.S. Chesman, C.H.O. Vane, J. Mar. Biol. Assoc. U. K. 85 (2005) 1.
[18] H. Hamid, C. Eskicioglu, Water Res. 46 (2012) 5813.
[19] T. Reports, J. Environ. Qual. 43 (2014) 568.
[20] Z. Yan, G. Lu, J. Liu, S. Jin, Z. Bay, Ecotox. Environ. Safe. 84 (2012) 334.
[21] A.R. Schwindt, D.L. Winkelman, K. Keteles, M. Murphy, A.M. Vajda, J. Appl. Ecol. 51 (2014) 582.
[22] R. Kralchevska, M. Milanova, Reac. Kinet. Mech. Cat. 109 (2013) 355.
[23] Z. Frontistis, C. Drosou, K. Tyrovola, D. Mantzavinos, D. Fatta-kassinos, D. Venieri, N.P. Xekoukoulotakis, Ind. Eng. Chem. Res. 51 (2012) 16552.
[24] J. Du, Y. Fan, W. Hu, L. Gu, X. Qian, Fresenius Environ. Bull. 21 (2012) 3515.
[25] M.C. Kanan, S. Kanan, H. Patterson, Res. Chem. Intermediat. 29 (2003) 691.
[26] S.M. Kanan, M.C. Kanan, H.H. Patterson, J. Phys. Chem. B 105 (2001) 7508.
[27] M. Bosco, M.P. Callao, M.S. Larrechi, Talanta 72 (2007) 800.
[28] G.J. Hall, J.E. Kenny, Anal. Chim. Acta 581 (2007) 118.
[29] G.J. Hall, K.E. Clow, J.E. Kenny, Environ. Sci. Technol. 39 (2005) 7560.
[30] R.M. Maggio, P.C. Damiani, A.C. Olivieri, Anal. Chim. Acta 677 (2010) 97.
[31] M. Alostaz, J. Environ. Eng. Sci. (2008) 183.
[32] D.J. Beale, N. a Porter, F. a Roddick, Water Sci. Technol. 67 (2013) 2428.
[33] S.-H. Zhu, H.-L. Wu, A.-L. Xia, Q.-J. Han, Y. Zhang, R.-Q. Yu, Talanta 74 (2008) 1579.
[34] R.D. JiJi, G.G. Andersson, K.S. Booksh, J. Chemometrics 14 (2000) 171.
[35] M.V. Bosco, M. Garrido, M.S. Larrechi, Anal. Chim. Acta 559 (2006) 240.
[36] D. Loeffler, M. Ramil, T. Ternes, M. Suter, R. Schönenberger, H. Aerni, K.S.A. Besa, Food Environ. (2010) 1.
[37] M. Mei, Z. Du, R. Xu, Y. Chen, H. Zhang, S. Qu, J. Hazard. Mater. 221–222 (2012) 100.
[38] L.N. Vandenberg, R. Hauser, M. Marcus, N. Olea, W.V. Welshons, Reprod. Toxicol. 24 (2007) 139.

[39] M.M. Schultz, E.T. Furlong, D.W. Kolpin, S.L. Werner, H.L. Schoenfuss, L.B. Barber, V.S. Blazer, D.O. Norris, A.M. Vajda, Environ. Sci. Technol. 44 (2010) 1918.
[40] C. Desbrow, E.J. Routledge, G.C. Brighty, J.P. Sumpter, M. Waldock, Environ. Sci. Technol. 32 (1998) 1549.
[41] E. Keller, V. Kramer, Z. Naturforsch. 60b (2005) 1255.
[42] Z. Deng, F. Tang, A.J. Muscat, Nanotechnology 19 (2008) 295705.
[43] C. Tan, G. Zhu, M. Hojamberdiev, K. Okada, J. Liang, X. Luo, P. Liu, Y. Liu, Appl. Catal. B 152–153 (2014) 425.